# A STUDY OF PHI MESON YIELD IN 200 GEV/A AU+AU COLLISIONS AT RHIC

A Thesis

Submitted to the Faculty

of

Purdue University

by

Timothy H. Herston

In Partial Fulfillment of the

Requirements for the Degree

of

Master of Science

August 2003

# TABLE OF CONTENTS

# LIST OF TABLES

# LIST OF FIGURES

## ABSTRACT

Herston, Timothy H. M.S., Purdue University, August, 2003. A Study of Phi Meson Yield in 200 GeV/A Au+Au Collisions at RHIC . Major Professors: Andrew Hirsch, Rolf Scharenberg, and Fuqiang Wang.

Herein is reported the results of phi meson yields in Au+Au collisions at $\sqrt{s_{NN}}$=200 GeV and measurement of the mean value and width of the phi resonance peak at different centralities. The yields were largely in agreement with previous studies using different analysis methodology. No changes in the phi mass peak's mean value or width were observed.

# 1. INTRODUCTION

In the beginning, the universe was a hot dense state of matter, the quark-gluon plasma, or QGP for short. And as the universe expanded, and quarks moved farther apart, it became apparent that while they could not all stay together, they could not bear to be alone. So the laws of physics said, "Let there be hadronization." And the evening and the morning were the first $10\mu s$ [1].

This is how the universe is believed to have begun, yet physicists know little about quarks and gluons, the fundamental building blocks of hadrons, because they are not known to exist as free particles, except possibly in a quark-gluon plasma. Hence much of modern high energy nuclear physics today is focused on trying to recreate for a brief time this QGP that existed in the early universe so that its properties can be studied [1].

One facility at the forefront of that quest is the Relativistic Heavy Ion Collider, or RHIC, at Brookhaven National Laboratory in Upton, New York [2]. The complex is designed to speed beams of ions such as gold nuclei to 99.995% of the speed of light [3], travelling opposite in direction in two concentric rings where they can be collided head on at several interaction points. It is hoped that after such a collision, the ions leave behind a region of energy of such high density that a QGP is created which can be studied by the properties of the myriad particles which emerge as it expands and hadronizes.

One of the interaction points where these collisions take place and are measured is the STAR experiment, which stands for Solenoidal Tracker At RHIC [4]. It consists primarily of a large time projection chamber capable of measuring the tracks of charged particles accurately enough for particle identification and reconstruction of kinematic data in a high track density environment. The analysis put forth herein is based on data obtained by the STAR detector.

If RHIC is successful in creating a quark-gluon plasma, it is expected to exist for less than $10^{-23}s$ [3], with no quarks or gluons escaping as free particles, so detection requires looking for various possible signals that have been theorized. Among these is an enhancement in the production of hadrons containing $s$ or $\overline{s}$ quarks such as phi mesons and kaons as compared to those containing only $u$, $\overline{u}$, $d$, or $\overline{d}$ quarks such as pions [5]. This is due to the suppression of strange particle production in ordinary hadronic interactions due to the Okubo-Zweig-Iikuza (OZI) rule [6], which is not expected to apply to production in a QGP.

The possibility of detecting strangeness enhancement is one reason for studying the phi meson, but it is not the only reason. The phi meson is composed of an $s$ quark and an $\overline{s}$ quark and has a low cross-section of interaction with other hadrons, again due to the OZI rule. Thus its kinematic data may contain information about the QGP which other particles have lost due to rescattering by the time they are detected.

In addition to this, the phi meson may offer another signal of a quark-gluon plasma: a change in the phi mass peak's mean value and/or width from those measured at lower energies [7]. In general, composite particles are not limited solely to the two or three quarks, known as valence quarks, which identify them, but rather consist as well of a whole sea of quarks and antiquarks which pop in and out of existence from the vacuum as a result of the tremendous forces inside a hadron. These sea quarks contribute most of the mass of the hadron.

In a quark-gluon plasma, however, the quarks and gluons are not bound in large groups, so if an $s$ quark and an $\overline{s}$ quark bonded, even briefly, as a phi meson, there would be no sea quarks to contribute to the mass. The result is that any phi meson which forms and decays inside a QGP would have a smaller mass. It is unlikely that many such decays would be observed due to the interaction of the decay products with the plasma, but if a shift in the measured phi mass were observed, it would be a likely signal of a quark-gluon plasma.

The focus of this analysis, then, is on the phi meson. It will examine yields at different collisions centralities and explore any shift in the mean mass of the phi resonance peak.

# 2. ANALYSIS

Since the phi meson is uncharged, the STAR detector does not observe it directly, so reconstructing its kinematic properties requires measuring the kinematic properties of its charged decay products. The most prevalent decay branch for the phi meson is decay into a $K^+K^-$ pair which accounts for 49.2% of phi decays. Other decay modes into two charged particles without involving multibody kinematics occur very rarely and thus are difficult to use for analysis[5].

The steps then in analyzing the phi meson are as follows:

• Identify all possible charged kaons and retrieve momenta of each.

• Reconstruct the invariant mass of each $K^+K^-$ pair within each event for different rapidity and transverse momentum bins, and correct for detector acceptance and efficiency.

• Remove the combinatorial background using the mixed event technique.

• Fit resonances near expected phi mass to a Breit-Wigner distribution to obtain phi yield as a function of transverse momentum.

The data sample used in this analysis is about 1.8 million minimum bias events from the 2001 RHIC run at center of mass energy 200 GeV/A. For each event, it was required that the z-vertex position was within 25 cm of the center of the TPC. The distance of closest approach for each track was within 3 cm of the center of the beam pipe to insure that all tracks used originated from the collision itself rather than later interactions of particles with the pipe or detector matter. The number of hits in the detector was required to be at least 15 out of a possible 45.

The energy loss of the particles, $\frac{dE}{dx}$, was used for help in identifying kaons. A new variable, z, was defined as follows:

$$z = \ln\left(\frac{dE/dx_{track}}{\overline{dE/dx_{kaon}}}\right)$$

The value of $\overline{dE/dx_{kaon}}$ is the approximate Gaussian center of the kaon Bethe-Bloch distribution with respect to $P_\perp$ [8]. With this definition, we required $|z| \leq 0.3$ which corresponds to about $3\sigma$ for the kaon distribution with respect to z. This cut eliminates many of the other particles at very low momentum and thus some of the background, but it becomes ineffective at higher momentum. It is not necessary to completely separate the kaons from other particles for this analysis, however, because the contribution to the background from these particles is essentially removed when the mixed event background is subtracted.

All tracks surviving the cuts to this point are treated as kaons and subjected to the following further cuts:

•$|y| < 1.0$

•$|P_\perp| < 5.0\ GeV/c$

where $y$ is the rapidity and $P_\perp$ is the transverse momentum.

The next step was to obtain the invariant mass for each $K^+K^-$ pair within each event for each $P_\perp$ bin. The invariant mass is defined as

$$M_{inv} = (E_{K^+} + E_{K^-})^2 - |\vec{p}_{K^+} + \vec{p}_{K^-}|^2$$

where the quantities E and $\vec{p}$ on the right refer to the kinetic energy and momentum respectively of the $K^+$ and $K^-$ in each pair. If any given pair were the product of a decay process, the invariant mass of the pair would correspond to the invariant mass or rest mass of the parent particle. Thus invariant mass histograms exhibit resonances around the known masses of parent particles with this decay mode, in the case of this analysis, the phi meson.

The invariant mass calculations are corrected by efficiency histograms derived from kaon embedding, thus the phi resonances obtained are corrected data rather than raw data. To obtain the efficiencies, Monte Carlo data is embedded in real data subject to the same potential loss of track hits as the real data and then put through the reconstruction process. The number of Monte Carlo tracks which can be successfully recovered divided by the number of tracks originally embedded is the efficiency. For this analysis the efficiency for kaons was fitted as a function of $P_\perp$ for several rapidity bins covering $|y| < 1.0$. The functional form used to fit the efficiency plots is:

$$\frac{A}{P_\perp} + Be^{-(\frac{C}{P_\perp})^D}$$

with A, B, C, and D acting as parameters for the fit.

The product of the efficiencies as a function of the kinematic variables of the daughters in a decay process is equal to the reconstruction efficiency of the parent. Thus weighting the invariant mass histograms by one over the product of the efficiencies of the $K^+$ and $K^-$ used in the calculation corrects the phi meson data.

This deviates from previous analyses in two ways. Previous analyses [9] applied corrections after raw phi meson yields were obtained, and phi embedding was used as the basis for the corrections. Correcting according to the kinematic quantities of the kaons and applying the corrections directly to the invariant mass for each pair eliminates the possibility of an invariant mass dependent correction and so allows investigation into whether the phi mass remains constant at different centralities, the results of which will be shown later.

The combinatorial background is eliminated by means of the mixed event method. That is if the positive kaons from one event and the negative kaons from a very similar event are used to make the invariant mass histograms described above, the shape of the combinatorial background is produced without any resonances since particles from different events can never come from the same decay process. These can be scaled to the size of the same event histograms and directly subtracted to leave only resonance decay distributions and a residual background due to other corelations in the same event, including Coulomb interactions.

In order to qualify as "very similar" events for mixing, the two events must have several things in common. They should be of the same centrality, originate from the same region in the TPC, and have the same reaction plane. To insure the first of these conditions, the events were separated into nine centrality classes according to charged particle multiplicity along divisions previously determined to correspond to a known percentage of events, and only events within each centrality were mixed. Within each centrality class, events were sorted by z-vertex position. This allowed selection of events which occured at nearly the same point to be used for the mixed event data. In order to have events with the same reaction plane, it was first necessary to determine the reaction plane of the events using data collected about the flow symmetry of the emerging particles. A rotation transformation was then done on the kaon momenta in each event so that all events had the same reaction plane with respect to the coordinate axes in which the kinematic data were measured. In order to meet all these analysis requirements, the data was scanned, and information was written to files in ASCII format, each line containing an event with the necessary event information and all candidate kaon information. With all these conditions met, the mixed event method very accurately reproduced the shape of the combinatorial background.

Finally the resonance peaks were fit to a Breit-Wigner function plus a linear background. The residual background was obtained from the best linear fit to the data in the region from $1.000 - 1.050$ $GeV/c^2$, excluding the points from $1.010 - 1.030$ $GeV/c^2$ to eliminate the phi peak itself from being included as background. The peaks were then fit to the function:

$$A \frac{B}{2\pi(m - m_\phi)^2 + \frac{B^2}{4}}$$

where $m_\phi$ is the mass of the phi meson as reported by the particle data group, and A and B are fit parameters with A representing the net phi yield.

## 3. RESULTS

Table 1 shows the values of $\frac{d^2N}{N_{events}2\pi P_{\perp}dP_{\perp}dy}$ $(GeV/c^2)^{-2}$ for four centralities in each $P_{\perp}$ bin for which a fit to the invariant mass peak could be obtained. Figures 1-4 show plots of these values as a function of $M_{\perp} - M_{\phi}$ for each of these centralities. The line through the points is the best fit to the function:

$$\frac{dN/dy}{2\pi T(T + M_{\phi})} e^{-(\frac{M_{\perp} - M_{\phi}}{T})}$$

where T and dN/dy are the fit parameters. The results of the fits are displayed in table 2 along with the results of previously published data [9] at the same energy and cuts using phi meson embedding to correct yields. As can be seen, the results are consistent for the three most central bins but show some discrepancy in the 50-80% bin. It is suspected that this is due to inadequate corrections at low $P_{\perp}$ stemming from poor statistics.

As has been previously discussed, this analysis allows investigation into whether a shift in the phi mass can be observed. Figures 5-8 are a fit to the phi peak in each of four centralities for $0.8GeV < P_{\perp} < 2.0GeV$ where the mass peak was allowed to act as a parameter in the fit. The parameters labeled P2 and P3 are parameters for the linear background. As is evident in the figures, the mean mass at each centrality is about 1.019 GeV, which is consistent with the phi mass reported by the particle data group, and the width is about 5 MeV, which is consistent with the reported 4 MeV with some additional smearing due to the momentum resolution of the detector. So no indication of a change in the mass peak can be inferred from this data.

The analysis presented here has been intended in part to verify previous results regarding phi meson yields using a different methodology and in part to explore a potential QGP signal related to the phi mass. As has been seen, the results produced by this analysis are generally consistent with those of the previous study. Indeed, if the points in the 50-80% centrality data that are most affected by the low statistics in the corrections are left out of the fit for the slope parameter and dN/dy, the fit becomes almost identical to the previous study.

In attempting to locate a signal of a quark-gluon plasma in the phi mass peak, this analysis should have found any detectable change, but none was seen. This does not mean that a QGP was not formed, however. It may be that such a signal is too weak to be observed. Many people are searching many possible signs in hopes of finding evidence of a new (or rather an old) state of matter, but no definitive proof has yet been found. There are tantalizing indications that the field is close, but for now physicists' understanding of the quark-gluon plasma is left where it started: in the beginning.

Table 3.1
$\frac{d^2N}{N_{events}2\pi P_\perp dP_\perp dy}$ $(GeV/c^2)^{-2}$ for four centralities. Statistical errors only.

| $P_\perp$ | Centrality | | | |
|---|---|---|---|---|
| $(GeV)$ | 0-10% | 10-30% | 30-50% | 50-80% |
| 0.6-0.8 | (9.76±0.55)E-1 | (6.51±0.21)E-1 | (2.50±0.09)E-1 | (4.54±0.23)E-2 |
| 0.8-1.0 | (7.06±0.45)E-1 | (3.54±0.15)E-1 | (1.72±0.08)E-1 | (3.46±0.21)E-2 |
| 1.0-1.2 | (4.31±0.42)E-1 | (2.74±0.17)E-1 | (1.19±0.08)E-1 | (2.43±0.23)E-2 |
| 1.2-1.4 | (3.96±0.38)E-1 | (1.80±0.17)E-1 | (1.01±0.08)E-1 | (2.26±0.21)E-2 |
| 1.4-1.6 | (2.23±0.27)E-1 | (1.51±0.14)E-1 | (6.54±0.65)E-2 | (1.45±0.16)E-2 |
| 1.6-1.8 | (1.64±0.23)E-1 | (8.49±0.99)E-2 | (3.32±0.51)E-2 | (7.28±1.27)E-3 |
| 1.8-2.0 | (3.25±1.01)E-2 | (4.07±0.59)E-2 | (1.31±0.28)E-2 | (4.35±0.86)E-3 |
| 2.0-2.2 | | (1.24±0.34)E-2 | (4.33±1.44)E-3 | (3.36±0.55)E-3 |
| 2.2-2.4 | (1.57±0.50)E-2 | (1.51±0.28)E-2 | (9.76±1.70)E-3 | (1.04±0.401)E-3 |
| 2.4-2.6 | (3.76±0.79)E-2 | (2.96±1.15)E-3 | (3.42±0.85)E-3 | (1.52±0.31)E-3 |
| 2.6-2.8 | | (2.99±1.10)E-3 | (5.50±1.00)E-3 | |
| 2.8-3.0 | | (4.07±0.89)E-3 | (1.51±0.46)E-3 | (3.41±1.14)E-4 |
| 3.0-3.2 | | | (1.49±0.38)E-3 | (2.94±1.06)E-4 |
| 3.2-3.4 | | | (8.91±3.81)E-4 | |
| 3.4-3.6 | | | (5.88±2.14)E-4 | (1.91±0.49)E-4 |

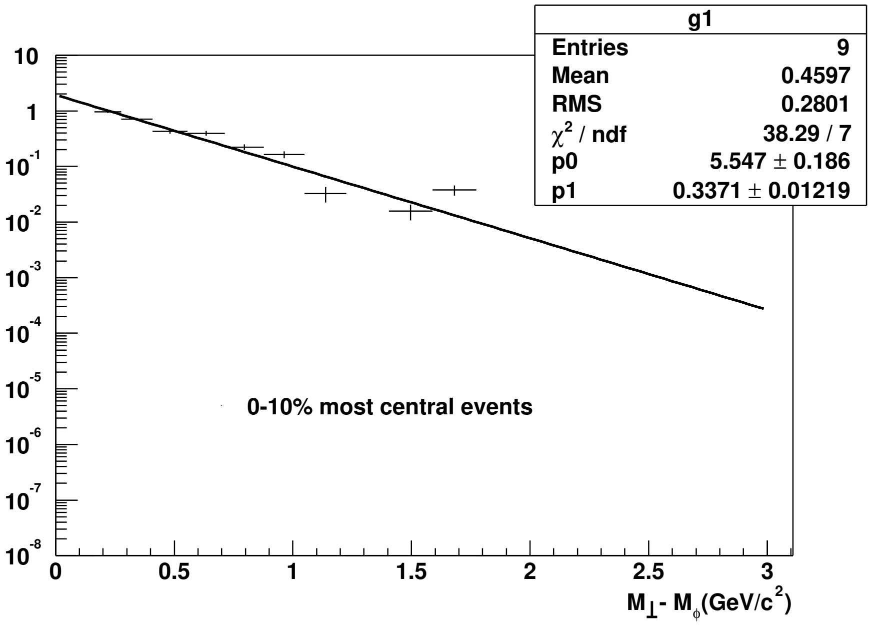


Figure 3.1.

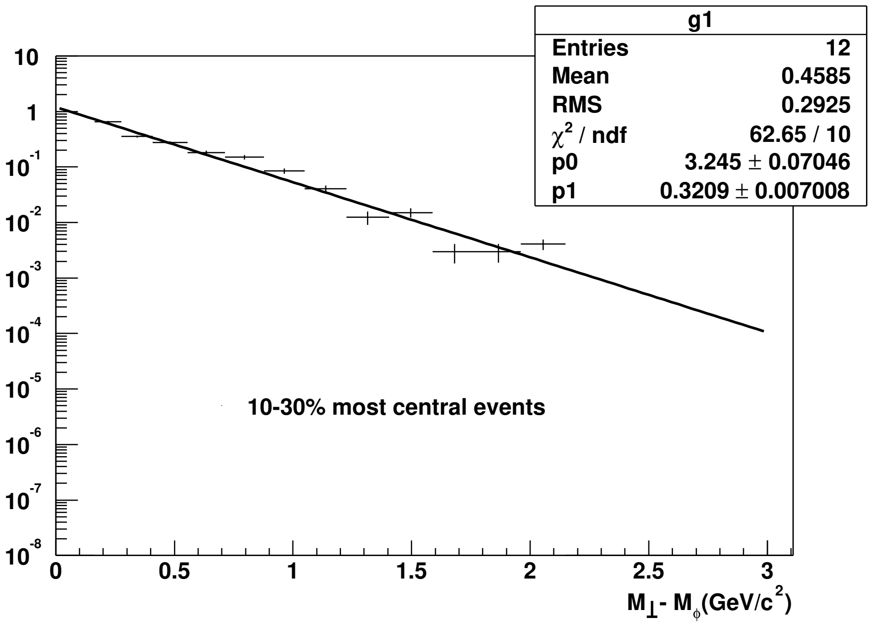


Figure 3.2.

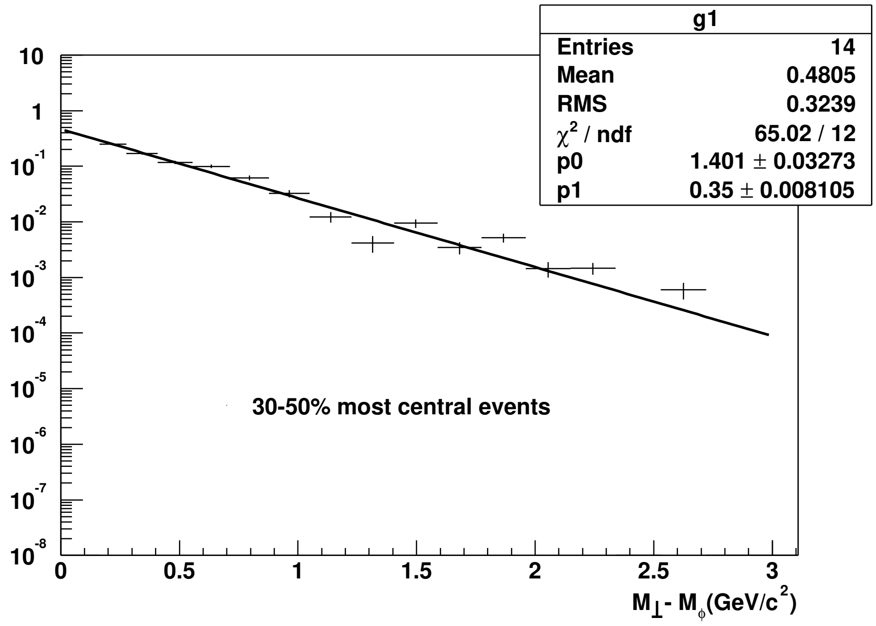


Figure 3.3.

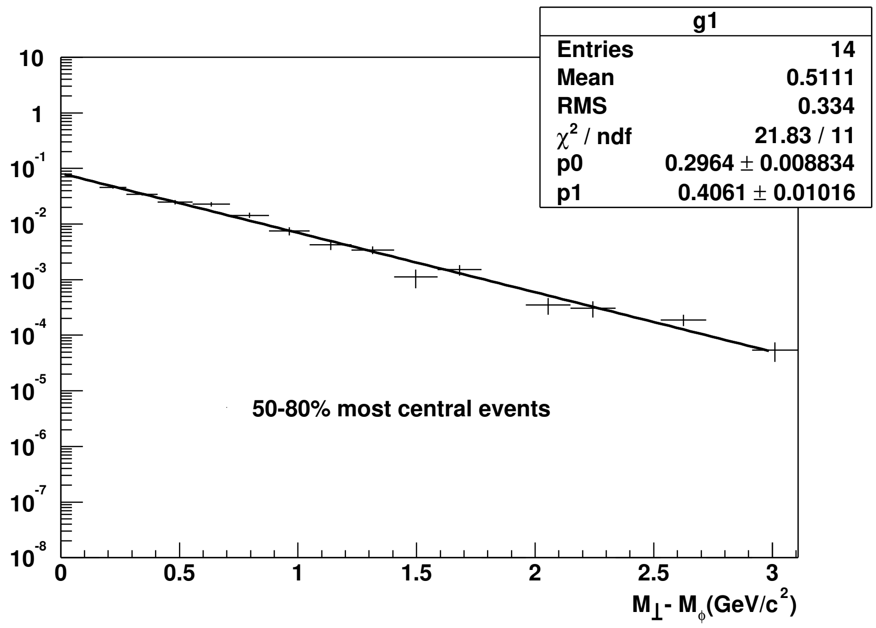


Figure 3.4.

Table 3.2
Slope parameters T and extrapolated yield dN/dy for above fits.

| Results of this analysis, ± stat | | |
|---|---|---|
| Event Centrality | Slope Parameter T ($MeV$) | dN/dy ($\|y\| < 0.5$) |
| 0-10% | 318 ± 11 | 6.1 ± 0.2 |
| 10-30% | 321 ± 7 | 3.2 ± 0.1 |
| 30-50% | 355 ± 8 | 1.4 ± 0.03 |
| 50-80% | 404 ± 10 | 0.29 ± 0.01 |
| Results of previous study, ± stat $^{+syst}_{-syst}$ | | |
| Event Centrality | Slope Parameter T ($MeV$) | dN/dy ($\|y\| < 0.5$) |
| 0-10% | $322 \pm 20^{+25}_{-10}$ | $5.9 \pm 0.5^{+1.0}_{-0.4}$ |
| 10-30% | $337 \pm 16^{+20}_{-20}$ | $3.4 \pm 0.2^{+0.5}_{-0.3}$ |
| 30-50% | $375 \pm 16^{+10}_{-50}$ | $1.4 \pm 0.1^{+0.2}_{-0.1}$ |
| 50-80% | $334 \pm 15^{+10}_{-40}$ | $0.40 \pm 0.02^{+0.08}_{-0.02}$ |

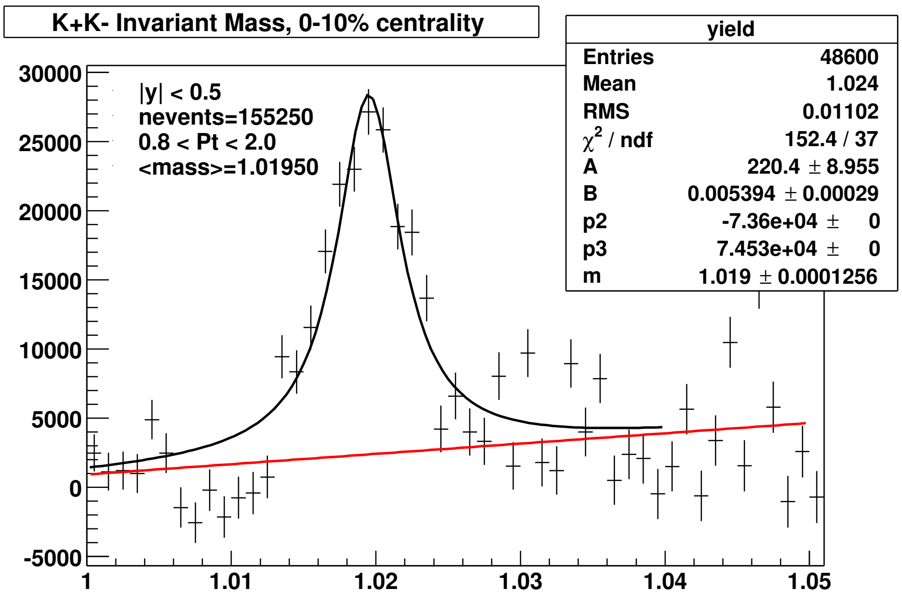


Figure 3.5. 0-10% most central events

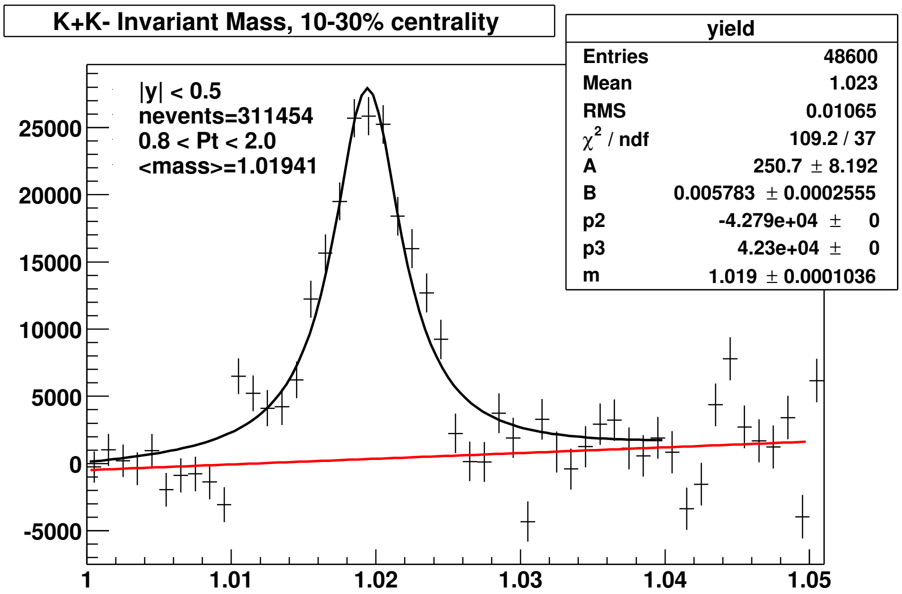


Figure 3.6. 10-30% most central events

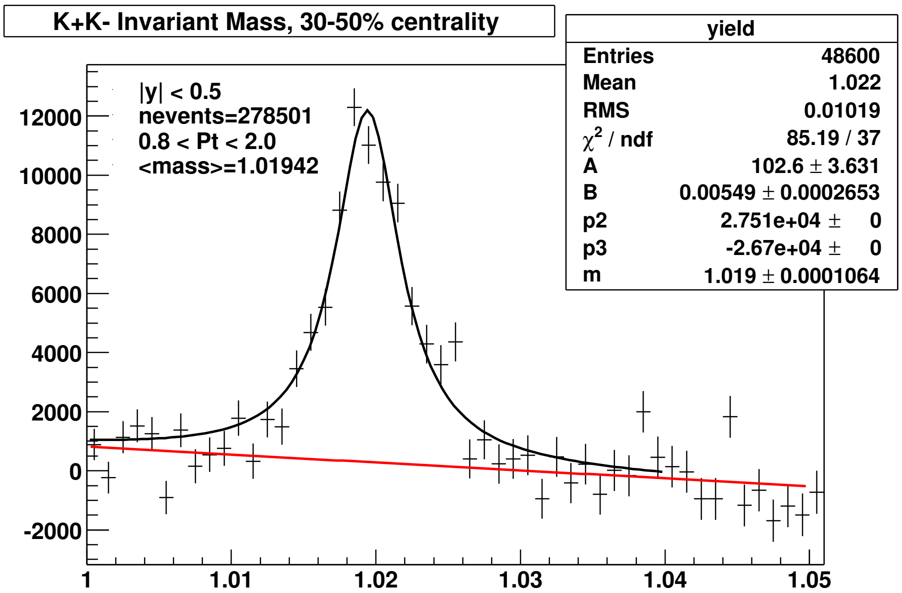


Figure 3.7. 30-50% most central events

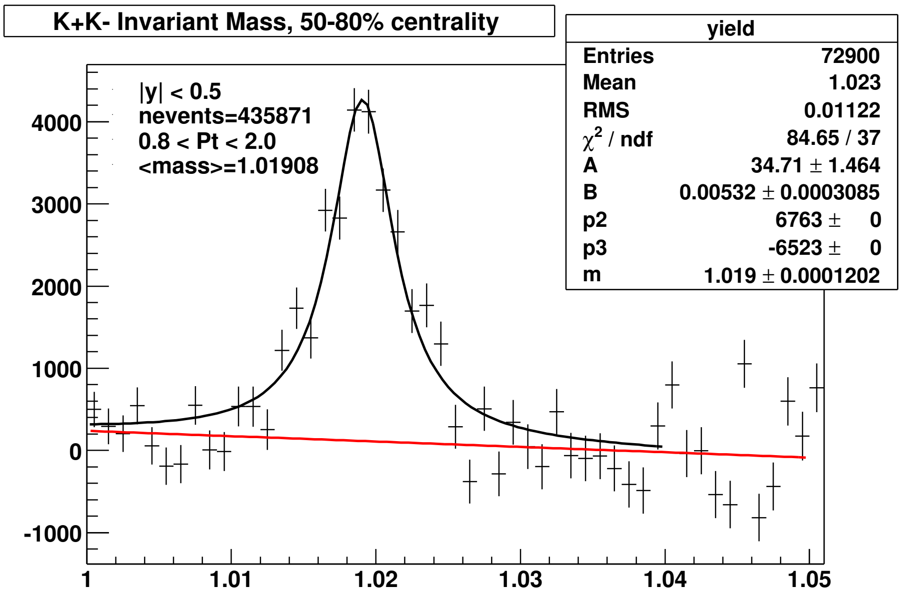


Figure 3.8. 50-80% most central events